Maximum-Likelihood Noncoherent PAM Detection

Dimitris S. Papailiopoulos, *Student Member, IEEE,* Georgina Abou Elkheir, and George N. Karystinos, *Member, IEEE*

***Abstract*—Sequence detection offers improved error-rate performance over conventional symbol-by-symbol detection when channel knowledge is not available at the receiver end. However, maximum-likelihood (ML) noncoherent sequence detection is proven to be notoriously intractable in many communication settings. In this work, we develop a new ML sequence detector for pulse-amplitude modulation (PAM) or quadrature-amplitude modulation (QAM) transmissions in unknown Rayleigh fading. Our detector identifies the ML sequence with overall polynomial complexity. This is possible via an auxiliary-angle approach that unlocks a low-rank property of the ML detection problem, reduces the exponential-size set of solution sequences to a polynomial-size set of candidates, and guarantees that the ML sequence is always contained in this substantially smaller set.**

***Index Terms*—Fading channels, lattice decoding, maximum likelihood decoding, noncoherent detection, sequence detection, wireless communications.**

I. Introduction

NONCOHERENT signal detection over unknown fading channels has received significant attention, in particular for the case of the block-fading channel model [1], [2]. The fact that channel knowledge is not used by noncoherent detectors to operate renders them applicable even to degraded and fast-fading channel settings. In [3], it was shown that conventional transmission schemes, such as phase-shift keying (PSK) or QAM, suffice to approach capacity in the single-input single-output (SISO) block Rayleigh-fading channel.

The major difference between coherent and noncoherent detection is the fact that, in the latter, the lack of channel knowledge induces memory in the received data sequence. Hence, to minimize the sequence error probability under this scenario, we need to perform ML sequence detection on the *entire* coherence interval. ML noncoherent sequence detection offers significant performance gains over conventional symbol-by-symbol (i.e., 1-lag) noncoherent detection [4]-[6], however, in general, it can be a notoriously hard problem due to its exponential complexity in the sequence length.

Interestingly, ML sequence detection does not always require exponential complexity. For example, if the data symbols take values from a PSK constellation, then ML noncoherent sequence detection under Rayleigh fading can be performed with complexity $\mathcal{O}(N \log N)$, where N is the sequence length, using the auxiliary-angle approach that was first presented in [7] and later used in [8]-[10]. However, the approach in [7] is restricted to constant-amplitude constellations. PAM and QAM are nonconstant-amplitude constellations, making noncoherent sequence detection more challenging.

Several attempts have been made in the direction of polynomial-complexity noncoherent PAM/QAM sequence detection. Generalized-likelihood-ratio-test (GLRT) detection algorithms of complexity $\mathcal{O}(N \log N)$ were developed in [11] for QAM transmissions over a phase-noncoherent, amplitude-coherent channel and in [12] for PAM transmissions over a phase-coherent, amplitude-noncoherent channel. The developments in [12] used lattice decoding techniques and also included an algorithm for GLRT PAM/QAM sequence detection over a fully noncoherent channel with complexity $\mathcal{O}\left(N^3\right)$ which was further reduced to $\mathcal{O}\left(N^2 \log N\right)$ in [13]. However, the question of whether ML noncoherent detection of a PAM/QAM sequence can also be performed in polynomial time or not has remained open.

In this work, we develop a method for ML noncoherent detection of M-PAM/QAM[1] symbol sequences under Rayleigh fading whose complexity is polynomial in the sequence length when M is constant. Our approach decomposes the detection problem into a polynomial-size set of simple problems. This is possible through an auxiliary-angle approach which, in principle, rephrases a computationally hard exhaustive-search problem into one that has to run on a polynomial-size search set. We show that this new set is built with polynomial complexity in the sequence length and always contains the ML PAM/QAM sequence. Interestingly, our approach gives a polynomial-complexity solution to a more general family of optimization problems which includes both ML and GLRT detection of a PAM/QAM sequence as special cases.

The rest of the paper is organized as follows. The problem formulation is presented in Section II where, to keep the presentation simple, we focus on PAM transmissions. The proposed method for the ML noncoherent detection of a PAM sequence is described in Section III and it is shown that its worst-case complexity is polynomial in the sequence length. In

Manuscript received June 27, 2012; revised September 30, 2012. The associate editor coordinating the review of this paper and approving it for publication was L. Szczecinski.

This work was supported in part by the Ministry of National Education of Greece under Thales Program Grant MIS-379418-DISCO. This paper was presented in part at the IEEE International Conference on Communications, Communication Theory Symposium, Ottawa, ON, June 2012.

D. S. Papailiopoulos is with the Department of Electrical Engineering, University of Southern California, Los Angeles, CA 90089 USA (e-mail: papailio@usc.edu).

G. Abou Elkheir was with the Department of Electronic and Computer Engineering, Technical University of Crete, Chania, 73100, Greece. She is now with the Department of Digital Systems, University of Piraeus, Piraeus, 18534, Greece (e-mail: georgina@unipi.gr).

G. N. Karystinos is with the Department of Electronic and Computer Engineering, Technical University of Crete, Chania, 73100, Greece (e-mail: karystinos@telecom.tuc.gr).

Digital Object Identifier 10.1109/TCOMM.2012.010913.120448

[1]Our method applies to QAM constellations with independent in-phase and quadrature components. In this work, the term QAM refers to solely such constellations.

Section IV, we show how the proposed technique is extended to QAM without increasing its worst-case complexity order. The performance of the proposed algorithm is tested through simulations in Section IV. A few concluding remarks are drawn in Section V.

II. Signal Model and Problem Statement

We consider a SISO system and assume transmission of a sequence of N uncoded M-ary PAM (M-PAM) data symbols $\mathbf{s} = [s_1, s_2, \ldots, s_N]^T$ where s_n, $n = 1, 2, \ldots, N$, is selected from an M-ary real-valued alphabet

$$\mathcal{A}_M \triangleq \left\{\pm a_1, \pm a_2, \ldots, \pm a_{\frac{M}{2}}\right\} \tag{1}$$

where $0 < a_1 < a_2 < \ldots < a_{\frac{M}{2}}$.[2] The data sequence is shaped, upconverted, and transmitted over a Rayleigh fading channel whose coherence length is at least N. The downconverted and pulse-matched filtered received vector is

$$\mathbf{y} = h\mathbf{s} + \mathbf{n} \tag{2}$$

where $h \sim \mathcal{CN}\left(0, \sigma_h^2\right)$ represents Rayleigh flat fading "channel processing" and $\mathbf{n} \sim \mathcal{CN}\left(\mathbf{0}, \sigma_n^2\mathbf{I}\right)$ denotes zero-mean additive white complex Gaussian noise.

Here, we assume that the channel coefficient h is not available to the receiver. Therefore, coherent detection cannot be utilized and the optimal, in terms of sequence error rate, receiver takes the form of a sequence detector that operates on the entire received vector $\mathbf{y}$.[3] Given the observation vector $\mathbf{y}$, the ML detector for the M-PAM sequence $\mathbf{s}$ maximizes the conditional probability density function (pdf) of $\mathbf{y}$ given $\mathbf{s}$. Thus, the optimal decision is given by

$$\mathbf{s}^{\text{ML}} = \underset{\mathbf{s}\in\mathcal{A}_M^N}{\arg\max}\, f\left(\mathbf{y}|\mathbf{s}\right) \tag{3}$$

where $f(\cdot|\cdot)$ represents the pertinent vector pdf of the channel output conditioned on the transmitted symbol sequence. The conditional received vector $\mathbf{y}$ given the transmitted sequence $\mathbf{s}$ is a complex Gaussian vector with mean $E\{\mathbf{y}|\mathbf{s}\} = \mathbf{0}$ and covariance matrix

$$\mathbf{C}_{\mathbf{y}|\mathbf{s}} \triangleq E\left\{\mathbf{y}\mathbf{y}^H|\mathbf{s}\right\} = \sigma_h^2\mathbf{s}\mathbf{s}^T + \sigma_n^2\mathbf{I}_N. \tag{4}$$

Therefore, the ML optimization problem in (3) is rewritten as

$$\mathbf{s}^{\text{ML}} = \underset{\mathbf{s}\in\mathcal{A}_M^N}{\arg\max}\, \frac{1}{\left|\mathbf{C}_{\mathbf{y}|\mathbf{s}}\right|}\exp\left(-\mathbf{y}^H\mathbf{C}_{\mathbf{y}|\mathbf{s}}^{-1}\mathbf{y}\right). \tag{5}$$

Using identities for the determinant and inverse of a rank-1 update [14], we compute

$$\begin{aligned}\left|\mathbf{C}_{\mathbf{y}|\mathbf{s}}\right| &= \left|\sigma_n^2\mathbf{I}_N + \sigma_h^2\mathbf{s}\mathbf{s}^T\right| = \left|\sigma_n^2\mathbf{I}_N\right|\left(1 + \frac{\sigma_h^2}{\sigma_n^2}\|\mathbf{s}\|^2\right) \\ &= \sigma_n^{2N-2}\left(\sigma_n^2 + \sigma_h^2\|\mathbf{s}\|^2\right)\end{aligned} \tag{6}$$

and

$$\mathbf{C}_{\mathbf{y}|\mathbf{s}}^{-1} = \left(\sigma_n^2\mathbf{I}_N + \sigma_h^2\mathbf{s}\mathbf{s}^T\right)^{-1} = \frac{1}{\sigma_n^2}\mathbf{I}_N - \frac{\sigma_h^2}{\sigma_n^4 + \sigma_h^2\sigma_n^2\|\mathbf{s}\|^2}\mathbf{s}\mathbf{s}^T. \tag{7}$$

[2]In this work, we need not specify $a_1, a_2, \ldots, a_{\frac{M}{2}}$ but only let them take arbitrary different positive values. In conventional M-PAM, the positive elements of $\mathcal{A}_M$ are given by $a_m = 2m - 1$, $m = 1, 2, \ldots, \frac{M}{2}$.

[3]In the following, for brevity, we refer to sequence-error-rate optimal detection simply as optimal.

If we substitute (6) and (7) in (5), we obtain

$$\begin{aligned}\mathbf{s}^{\text{ML}} &= \underset{\mathbf{s}\in\mathcal{A}_M^N}{\arg\max}\Bigg\{-\mathbf{y}^H\left(\frac{1}{\sigma_n^2}\mathbf{I}_N - \frac{\sigma_h^2}{\sigma_n^4 + \sigma_h^2\sigma_n^2\|\mathbf{s}\|^2}\mathbf{s}\mathbf{s}^T\right)\mathbf{y} \\ &\qquad - \ln\left(\sigma_n^{2N-2}\left(\sigma_n^2 + \sigma_h^2\|\mathbf{s}\|^2\right)\right)\Bigg\} \\ &= \underset{\mathbf{s}\in\mathcal{A}_M^N}{\arg\max}\Bigg\{\frac{\sigma_h^2}{\sigma_n^2(\sigma_h^2\|\mathbf{s}\|^2 + \sigma_n^2)}\left|\mathbf{y}^H\mathbf{s}\right|^2 \\ &\qquad - \ln\left(\sigma_h^2\|\mathbf{s}\|^2 + \sigma_n^2\right)\Bigg\} \\ &= \underset{\mathbf{s}\in\mathcal{A}_M^N}{\arg\max}\Big\{g_{\text{ML}}(\|\mathbf{s}\|)\left\|\mathbf{V}^T\mathbf{s}\right\|^2 + h_{\text{ML}}(\|\mathbf{s}\|)\Big\}\end{aligned} \tag{8}$$

where $g_{\text{ML}}(x) \triangleq \frac{\sigma_h^2}{\sigma_n^2(\sigma_h^2x^2+\sigma_n^2)}$, $h_{\text{ML}}(x) \triangleq -\ln(\sigma_h^2x^2 + \sigma_n^2)$, and $\mathbf{V} \triangleq [\Re\{\mathbf{y}\}\ \Im\{\mathbf{y}\}]$ where $\Re\{\mathbf{y}\}$ and $\Im\{\mathbf{y}\}$ denote the real and imaginary, respectively, parts of vector $\mathbf{y}$.

If, on the other hand, we consider joint channel estimation and data detection, then the GLRT rule [12], [13]

$$\begin{aligned}\mathbf{s}^{\text{GLRT}} &= \underset{\mathbf{s}\in\mathcal{A}_M^N}{\arg\min}\left\{\min_{h\in\mathbb{C}}\|\mathbf{y} - h\mathbf{s}\|\right\} = \underset{\mathbf{s}\in\mathcal{A}_M^N}{\arg\min}\left\|\mathbf{y} - \frac{\mathbf{s}^T\mathbf{y}}{\|\mathbf{s}\|^2}\mathbf{s}\right\| \\ &= \underset{\mathbf{s}\in\mathcal{A}_M^N}{\arg\max}\,\frac{\left|\mathbf{y}^H\mathbf{s}\right|^2}{\|\mathbf{s}\|^2}\end{aligned} \tag{9}$$

can, similarly to (8), take the form

$$\mathbf{s}^{\text{GLRT}} = \underset{\mathbf{s}\in\mathcal{A}_M^N}{\arg\max}\left\{g_{\text{GLRT}}(\|\mathbf{s}\|)\left\|\mathbf{V}^T\mathbf{s}\right\|^2 + h_{\text{GLRT}}(\|\mathbf{s}\|)\right\} \tag{10}$$

by setting $g_{\text{GLRT}}(x) \triangleq \frac{1}{x^2}$ and $h_{\text{GLRT}}(x) \triangleq 0$.

Hence, both the ML optimization problem in (5) and the GLRT optimization problem in (9) are special cases of the more general optimization problem

$$\boxed{\begin{array}{l}\mathcal{P}: \\ \quad\displaystyle\max_{\mathbf{s}\in\mathcal{A}_M^N}\left\{g(\|\mathbf{s}\|)\left\|\mathbf{V}^T\mathbf{s}\right\|^2 + h(\|\mathbf{s}\|)\right\}\end{array}} \tag{11}$$

where $g : \mathbb{R} \to \mathbb{R}^+$, $h : \mathbb{R} \to \mathbb{R}$, and $\mathbf{V} \in \mathbb{R}^{N\times 2}$. A straightforward approach to solve $\mathcal{P}$ would be an exhaustive search among all M^N sequences $\mathbf{s} \in \mathcal{A}_M^N$. However, such a solver would be impractical even for moderate values of N, since its complexity grows exponentially with N. In the next section, we present an efficient algorithm that solves $\mathcal{P}$ in polynomial time for any $g : \mathbb{R} \to \mathbb{R}^+$, $h : \mathbb{R} \to \mathbb{R}$, and $\mathbf{V} \in \mathbb{R}^{N\times 2}$.

III. Polynomial-complexity ML PAM Sequence Detection

The main contribution of this work is stated in the following proposition.

Proposition 1: Problem $\mathcal{P}$ is solvable with complexity $\mathcal{O}\left(N^{\frac{M}{2}+1}\right)$. □

We follow a proof-by-construction which we decompose into three parts. First, we show that $\mathcal{P}$ is equivalent to a union of subproblems whose number is polynomial in N. Then, we show that, for each subproblem, we can identify a set of candidate solutions which has cardinality polynomial in N

and can be built in time polynomial in N. The solution of $\mathcal{P}$ is always in this ensemble of candidate sets, implying that the aggregate complexity to solve $\mathcal{P}$ is polynomial in N.

A. A polynomial number of subproblems

We begin our developments by defining the set of positive amplitudes of the elements of $\mathcal{A}_M$,

$$\mathcal{A}_M^+ \triangleq \left\{a_1, a_2, \ldots, a_{\frac{M}{2}}\right\}, \tag{12}$$

and rewriting $\mathbf{s} \in \mathcal{A}_M^N$ as

$$\mathbf{s} = \mathbf{b} \odot \mathbf{x} \tag{13}$$

where $\mathbf{b} \in \left(\mathcal{A}_M^+\right)^N$ is the amplitude component of $\mathbf{s}$ and has the same norm as $\mathbf{s}$, i.e., $\|\mathbf{b}\| = \|\mathbf{s}\|$, $\mathbf{x} \in \{\pm 1\}^N$ is the sign component of $\mathbf{s}$, and $\odot$ accounts for Hadamard (i.e., entry-wise) product. We can now rewrite $\mathcal{P}$ in (11) as

$$\begin{aligned}&\max_{\mathbf{b}\in\left(\mathcal{A}_M^+\right)^N} \max_{\mathbf{x}\in\{\pm1\}^N} \left\{g(\|\mathbf{b}\|) \left\|\mathbf{V}^T\left(\mathbf{b}\odot\mathbf{x}\right)\right\|^2 + h(\|\mathbf{b}\|)\right\}\\ &= \max_{\mathbf{b}\in\left(\mathcal{A}_M^+\right)^N} \left\{g(\|\mathbf{b}\|) \max_{\mathbf{x}\in\{\pm1\}^N} \left\|\mathbf{V}^T\left(\mathbf{b}\odot\mathbf{x}\right)\right\|^2 + h(\|\mathbf{b}\|)\right\}.\end{aligned} \tag{14}$$

Hence, instead of searching for the optimal vector $\mathbf{s} \in \mathcal{A}_M^N$ in (11), we equivalently search for the optimal amplitude-sign vector pair $(\mathbf{b}, \mathbf{x}) \in \left(\mathcal{A}_M^+\right)^N \times \{\pm 1\}^N$ in (14). In the following, we see that this amplitude-sign decomposition is fundamental to observe that the problem can be solved efficiently.

The main idea that we exploit and which eventually leads to a tractable and efficient algorithm is the following. If we fix the type [15] of sequence $\mathbf{b}$ (i.e., the frequency of appearance of the elements of $\mathcal{A}_M^+$ in $\mathbf{b}$), then the norm of $\mathbf{b}$ is also fixed and the double maximization problem in (14) reduces to a single maximization over $\mathbf{x} \in \{\pm 1\}^N$ which is solvable in polynomial time. Interestingly, the number of all possible types is polynomial in N, leading to a polynomial-time solution of (14).

To formulate our approach, we define function F which associates any vector $\mathbf{b} \in \left(\mathcal{A}_M^+\right)^N$ to its unnormalized type vector $\mathbf{t} = F(\mathbf{b}) \in \{0, 1, \ldots, N\}^{\frac{M}{2}}$. That is, the mth element t_m of $\mathbf{t} = F(\mathbf{b})$ equals the number of times of appearance of value a_m in $\mathbf{b}$, $m = 1, 2, \ldots, \frac{M}{2}$. Then, we partition $\left(\mathcal{A}_M^+\right)^N$ into disjoint sets $\mathcal{B}_1, \mathcal{B}_2, \ldots, \mathcal{B}_K$ so that each set $\mathcal{B}_k$ contains all vectors $\mathbf{b} \in \left(\mathcal{A}_M^+\right)^N$ with common type, say $\mathbf{t}_k$, and, hence, common norm, say β_k. That is,

$$\left(\mathcal{A}_M^+\right)^N = \bigcup_{k=1}^{K} \mathcal{B}_k \tag{15}$$

where, for any $k = 1, 2 \ldots, K$,

$$\mathcal{B}_k \triangleq \left\{\mathbf{b} \in \left(\mathcal{A}_M^+\right)^N : \; F(\mathbf{b}) = \mathbf{t}_k\right\} \tag{16}$$

and

$$\|\mathbf{b}\| = \beta_k, \quad \forall \; \mathbf{b} \in \mathcal{B}_k. \tag{17}$$

Apparently, the number K of all distinct types (hence, sets) equals the number of possible ways one can choose N elements of a set of $\frac{M}{2}$ elements, disregarding order and allowing repeated elements, and is given by [16]

$$K = \left(\!\!\binom{M/2}{N}\!\!\right) = \binom{\frac{M}{2} + N - 1}{N}. \tag{18}$$

Interestingly, $K = \mathcal{O}\left(N^{\frac{M}{2}-1}\right)$ is polynomial in N.

Since we have partitioned $\left(\mathcal{A}_M^+\right)^N$ into K sets so that each set contains vectors with common type and norm, using (14) we can reexpress $\mathcal{P}$ as

$$\begin{aligned}&\max_{k=1,2,\ldots,K} \max_{\mathbf{b}\in\mathcal{B}_k} \left\{g(\|\mathbf{b}\|) \max_{\mathbf{x}\in\{\pm1\}^N} \left\|\mathbf{V}^T(\mathbf{b}\odot\mathbf{x})\right\|^2 + h(\|\mathbf{b}\|)\right\}\\ &= \max_{k=1,2,\ldots,K} \left\{g(\beta_k) \max_{\mathbf{b}\in\mathcal{B}_k} \max_{\mathbf{x}\in\{\pm1\}^N} \left\|\mathbf{V}^T(\mathbf{b}\odot\mathbf{x})\right\|^2 + h(\beta_k)\right\}.\end{aligned} \tag{19}$$

According to (19), to obtain the optimal pair $(\mathbf{b}, \mathbf{x}) \in \left(\mathcal{A}_M^+\right)^N \times \{\pm 1\}^N$, we can equivalently compute the optimal pair $(\mathbf{b}, \mathbf{x}) \in \mathcal{B}_k \times \{\pm 1\}^N$, for each $k = 1, 2, \ldots, K$. That is, we can focus on the inner maximization in (19),

$$\max_{\mathbf{b}\in\mathcal{B}_k} \max_{\mathbf{x}\in\{\pm1\}^N} \left\|\mathbf{V}^T(\mathbf{b}\odot\mathbf{x})\right\|^2, \tag{20}$$

or, simply, focus on

$$\boxed{\begin{aligned}&\mathcal{P}_k :\\ &\quad \max_{\mathbf{b}\in\mathcal{B}_k} \max_{\mathbf{x}\in\{\pm1\}^N} \left\|\mathbf{V}^T\left(\mathbf{b}\odot\mathbf{x}\right)\right\|\end{aligned}} \tag{21}$$

where $\mathbf{V} \in \mathbb{R}^{N\times 2}$. Hence, we have the following lemma.

Lemma 1: Solving the $K = \mathcal{O}\left(N^{\frac{M}{2}-1}\right)$ subproblems $\mathcal{P}_1, \mathcal{P}_2, \ldots, \mathcal{P}_K$ is sufficient to solve $\mathcal{P}$. □

In summary, to obtain the vector $\mathbf{s}$ that solves $\mathcal{P}$ in (11), we can equivalently solve $\mathcal{P}_k$ in (21) to obtain $(\mathbf{b}_k, \mathbf{x}_k)$ and create the corresponding vector $\mathbf{s}_k = \mathbf{b}_k \odot \mathbf{x}_k$, for each $k = 1, 2, \ldots, K$, and compare $\mathbf{s}_1, \mathbf{s}_2, \ldots, \mathbf{s}_K$ against the optimization metric in (11). Since K is polynomial in N, to prove polynomial solvability of $\mathcal{P}$ it suffices to show that $\mathcal{P}_k$ can be solved in polynomial time. The latter is proved in the following subsections by constructing efficiently a set of N^2 candidate vector pairs $(\mathbf{b}, \mathbf{x})$ which includes the solution of $\mathcal{P}_k$. In Fig. 1, we sketch the steps of our proof, where $\mathbf{s}^{(k,i)}$, $i = 1, 2, \ldots, N^2$, indicates a candidate solution of $\mathcal{P}_k$, $k = 1, 2, \ldots, K$.

B. Redefining the problem space

First, we define function *match* which assigns optimally, in a maximal-ratio-combining sense, an amplitude vector $\mathbf{b} \in \mathcal{B}_k$, $k = 1, 2, \ldots, K$, to an arbitrary vector $\mathbf{u} \in \mathbb{R}^N$, as follows.

$$\mathbf{b} = \text{match}(k; \mathbf{u}) \triangleq \arg\max_{\mathbf{b}\in\mathcal{B}_k} \mathbf{b}^T|\mathbf{u}|. \tag{22}$$

That is, $\text{match}(k; \mathbf{u})$ selects the amplitude vector $\mathbf{b} \in \mathcal{B}_k$ which maximizes its inner product with the magnitude of an arbitrary vector $\mathbf{u} \in \mathbb{R}^N$. It turns out that the outcome of $\text{match}(k; \mathbf{u})$ is a vector $\mathbf{b} \in \mathcal{B}_k$ that satisfies

$$b_n \geq b_l \Leftrightarrow |u_n| \geq |u_l|, \quad \forall \; n, l \in \{1, 2, \ldots, N\}. \tag{23}$$

We note that, for a given $k = 1, 2, \ldots, K$, all amplitude vectors $\mathbf{b} \in \mathcal{B}_k$ have a common type $\mathbf{t}_k = F(\mathbf{b})$. Then,

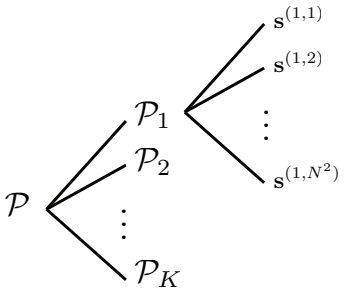

Fig. 1. A sketch of the steps of our proof. We first show that, instead of solving $\mathcal{P}$, we can concentrate on K subproblems $\mathcal{P}_1$, $\mathcal{P}_2$, ..., $\mathcal{P}_K$. Then, for each $k = 1, 2, \ldots, K$, we focus on subproblem $\mathcal{P}_k$ and identify N^2 candidate solution vectors $\mathbf{s}^{(k,1)}$, $\mathbf{s}^{(k,2)}$, ..., $\mathbf{s}^{(k,N^2)}$ in polynomial time. Finally, we show that the optimal solution to the initial problem $\mathcal{P}$, which includes the ML noncoherent PAM detection problem as a special case, belongs to the union of the aforementioned sets of candidates.

the computational cost of match$(k; \mathbf{u})$ is $\mathcal{O}(N \log N)$ through sorting the elements of $|\mathbf{u}|$ and assigning the $t_k(1)$ smallest values to a_1, the next $t_k(2)$ smallest values to a_2, and so on. In the developments that follow, *match* is critical in proving that $\mathcal{P}_k$ can be solved in polynomial time.

To solve $\mathcal{P}_k$, we introduce the angle $\phi \in (-\pi, \pi]$ and define the unit-norm polar 2×1 vector

$$\mathbf{c}(\phi) \stackrel{\triangle}{=} \begin{bmatrix} \sin(\phi) \\ \cos(\phi) \end{bmatrix}. \tag{24}$$

In the following, we will see that ϕ unlocks the low-rank structure of matrix $\mathbf{V}$ which is exploited to identify a polynomial number of *locally optimal* candidate amplitude-sign pairs $(\mathbf{b}, \mathbf{x})$. The optimal solution of $\mathcal{P}_k$ will be among the locally optimal ones.

Due to the unity of the norm of $\mathbf{c}(\phi)$, from Cauchy-Schwarz Inequality, we obtain, for any vector $\mathbf{a} \in \mathbb{R}^2$,

$$\mathbf{a}^T \mathbf{c}(\phi) \leq \|\mathbf{a}\| \underbrace{\|\mathbf{c}(\phi)\|}_{=1} = \|\mathbf{a}\|. \tag{25}$$

The equality above is achieved if and only if ϕ is the angle of $\mathbf{a}$ so that $\mathbf{c}(\phi)$ is codirectional with $\mathbf{a}$. If we substitute $\mathbf{a}$ with $\mathbf{V}^T(\mathbf{b} \odot \mathbf{x})$, then we obtain

$$\max_{\phi \in (-\pi, \pi]} \left\{ \left(\mathbf{b}^T \odot \mathbf{x}^T \right) \mathbf{V} \mathbf{c}(\phi) \right\} = \left\| \mathbf{V}^T (\mathbf{b} \odot \mathbf{x}) \right\|. \tag{26}$$

Therefore, $\mathcal{P}_k$ in (21) is equivalent to

$$\max_{\mathbf{b} \in \mathcal{B}_k} \max_{\mathbf{x} \in \{\pm 1\}^N} \max_{\phi \in (-\pi, \pi]} \left\{ \left(\mathbf{x}^T \odot \mathbf{b}^T \right) \mathbf{V} \mathbf{c}(\phi) \right\}. \tag{27}$$

If we set

$$\mathbf{u}(\phi) \stackrel{\triangle}{=} \mathbf{V} \mathbf{c}(\phi) = \begin{bmatrix} V_{1,1} \sin(\phi) + V_{1,2} \cos(\phi) \\ \vdots \\ V_{N,1} \sin(\phi) + V_{N,2} \cos(\phi) \end{bmatrix} \tag{28}$$

and change the order of the maximizations in (27), then $\mathcal{P}_k$ becomes

$$\begin{aligned} &\max_{\phi \in (-\pi, \pi]} \max_{\mathbf{b} \in \mathcal{B}_k} \max_{\mathbf{x} \in \{\pm 1\}^N} \left\{ \mathbf{x}^T \mathrm{diag}(\mathbf{b}) \mathbf{u}(\phi) \right\} \\ &= \max_{\phi \in (-\pi, \pi]} \max_{\mathbf{b} \in \mathcal{B}_k} \max_{\mathbf{x} \in \{\pm 1\}^N} \left\{ \mathbf{x}^T (\mathbf{b} \odot \mathbf{u}(\phi)) \right\}. \end{aligned} \tag{29}$$

For any given point $\phi \in (-\pi, \pi]$ and any given vector $\mathbf{b} \in \mathcal{B}_k$, the inner maximization in (29) is achieved for

$$\mathbf{x}(\phi) \stackrel{\triangle}{=} \mathrm{sgn}(\mathbf{b} \odot \mathbf{u}(\phi)) = \mathrm{sgn}(\mathbf{u}(\phi)), \tag{30}$$

resulting in the value

$$\max_{\mathbf{x} \in \{\pm 1\}^N} \left\{ \mathbf{x}^T (\mathbf{b} \odot \mathbf{u}(\phi)) \right\} = \mathbf{b}^T |\mathbf{u}(\phi)|. \tag{31}$$

Then, the optimal amplitude vector for the given $\phi \in (-\pi, \pi]$ is

$$\mathbf{b}_k(\phi) \stackrel{\triangle}{=} \arg\max_{\mathbf{b} \in \mathcal{B}_k} \mathbf{b}^T |\mathbf{u}(\phi)| = \mathrm{match}(k; \mathbf{u}(\phi)). \tag{32}$$

Since $\mathbf{c}(\phi + \pi) = -\mathbf{c}(\phi)$, we obtain $\mathbf{u}(\phi + \pi) = -\mathbf{u}(\phi) \Rightarrow |\mathbf{u}(\phi + \pi)| = |\mathbf{u}(\phi)|$. Hence, $\phi + \pi$ and ϕ are associated with equal amplitude vectors $\mathbf{b}_k(\phi + \pi) = \mathbf{b}_k(\phi)$ and opposite sign vectors $\mathbf{x}(\phi + \pi) = -\mathbf{x}(\phi)$, which implies that they result in the same metric value in $\mathcal{P}_k$ (cf. (21)). Therefore, in the following, we can ignore the values of $\phi \in \left(-\pi, -\frac{\pi}{2}\right] \cup \left(\frac{\pi}{2}, \pi\right]$ and restrict ϕ to the interval $\left(-\frac{\pi}{2}, \frac{\pi}{2}\right]$.

Notice that, for any $n = 1, 2, \ldots, N$,

$$u_n(\phi) = V_{n,1} \sin(\phi) + V_{n,2} \cos(\phi), \tag{33}$$

i.e., every element of $\mathbf{u}(\phi)$ is a continuous function, or a curve, of ϕ. When, due to (30), we examine the sign of $\mathbf{u}(\phi)$ at a given point ϕ, we actually examine the signs of the curves $u_1(\phi)$, $u_2(\phi)$, ..., $u_N(\phi)$ according to their values at ϕ. Similarly, when, due to (32), we sort the elements of $|\mathbf{u}(\phi)|$ at a given point ϕ (as function *match* requires), we actually sort the curves according to their magnitudes at point ϕ. The optimal pair $(\mathbf{b}_k, \mathbf{x}_k) \in \mathcal{B}_k \times \{\pm 1\}^N$ in (29), i.e., the solution of $\mathcal{P}_k$, is met if we scan the entire interval $\left(-\frac{\pi}{2}, \frac{\pi}{2}\right]$ and collect the locally optimal pair $(\mathbf{b}_k(\phi), \mathbf{x}(\phi))$ for any point $\phi \in \left(-\frac{\pi}{2}, \frac{\pi}{2}\right]$.

A natural question that arises is the following. How many sign and sorting subproblems are induced if we scan all values of $\phi \in \left(-\frac{\pi}{2}, \frac{\pi}{2}\right]$? An answer to the previous question identifies exactly the number of locally optimal solutions for $\mathcal{P}_k$.

The auxiliary angle ϕ now becomes relevant in answering the above question. Due to the continuity of the curves $u_i(\phi)$, we expect that in an area around ϕ the curves will retain their signs and magnitude sorting. Hence, we expect the formation of intervals in $\left(-\frac{\pi}{2}, \frac{\pi}{2}\right]$ within which both the signs and the magnitude sorting of the curves will remain unaltered, albeit the value of each curve is varying. To illustrate this, in Fig. 2, we set N to 3, consider an arbitrary 3×2 matrix $\mathbf{V}$, and plot curves $|u_1(\phi)|$, $|u_2(\phi)|$, and $|u_3(\phi)|$ versus $\phi \in \left(-\frac{\pi}{2}, \frac{\pi}{2}\right]$. We indicate some sign and magnitude sorting change examples explicitly. On the horizontal axis, we indicate the points where a curve changes sign and the points where two curves change their magnitude sorting. There are in total 9 sign and magnitude sorting changes which define a partition of $\left(-\frac{\pi}{2}, \frac{\pi}{2}\right]$ into 10 nonoverlapping intervals. Each such interval is associated with an amplitude-sign vector pair $(\mathbf{b}_k(\phi), \mathbf{x}(\phi))$ that remains unaltered when ϕ belongs to the corresponding interval, for any fixed value of $k = 1, 2, \ldots, K$. Below the plot of the curves, for any $\phi \in \left(-\frac{\pi}{2}, \frac{\pi}{2}\right]$, we explicitly show the locally optimal amplitude vector $\mathbf{b}_k(\phi)$, for any fixed value of $k = 1, 2, \ldots, K$, and the locally optimal sign vector $\mathbf{x}(\phi)$.

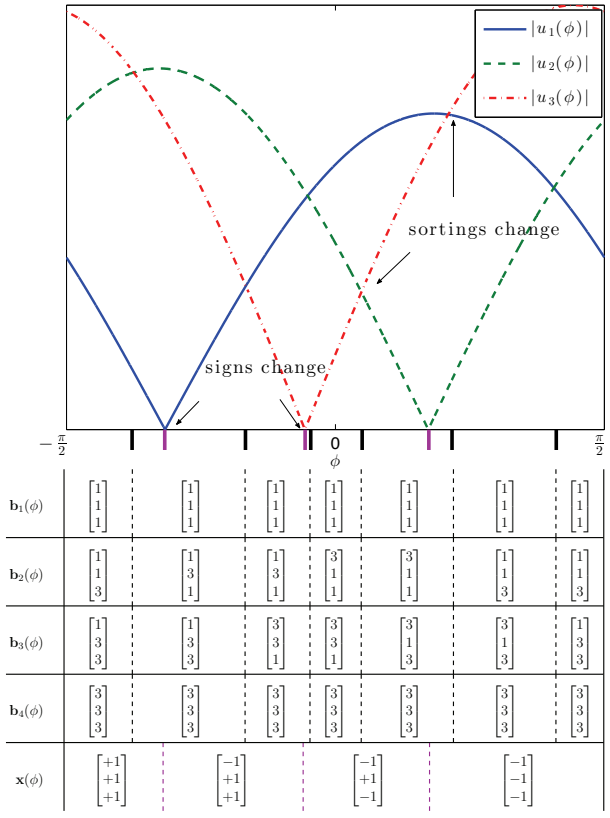

Fig. 2. Curves $|u_1(\phi)|$, $|u_2(\phi)|$, and $|u_3(\phi)|$ versus $\phi \in \left(-\frac{\pi}{2}, \frac{\pi}{2}\right]$, for an arbitrary 3×2 matrix $\mathbf{V}$ ($N = 3$). We indicate some sign and magnitude sorting change examples explicitly. On the horizontal axis, we indicate the points where a curve changes sign and the points where two curves change their magnitude sorting. There are in total 9 sign and magnitude sorting changes which define a partition of $\left(-\frac{\pi}{2}, \frac{\pi}{2}\right]$ into 10 nonoverlapping intervals. Each such interval is associated with an amplitude-sign vector pair $(\mathbf{b}_k(\phi), \mathbf{x}(\phi))$ that remains unaltered when ϕ belongs to the corresponding interval, for any fixed value of $k = 1, 2, \ldots, K$. Below the plot of the curves, for any $\phi \in \left(-\frac{\pi}{2}, \frac{\pi}{2}\right]$, we explicitly show the locally optimal amplitude vector $\mathbf{b}_k(\phi)$, for any fixed value of $k = 1, 2, \ldots, K$, and the locally optimal sign vector $\mathbf{x}(\phi)$.

In the sequel, we determine all these intervals, show that their number is less than or equal to N^2, and present a polynomial-time algorithm that identifies the pairs $(\mathbf{b}, \mathbf{x}) \in \mathcal{B}_k \times \{\pm 1\}^N$ that are associated with these intervals. Once we have collected all candidate pairs $(\mathbf{b}, \mathbf{x}) \in \mathcal{B}_k \times \{\pm 1\}^N$ for any $k = 1, 2, \ldots, K$, the solution of $\mathcal{P}$ in (11) is determined with the help of (13) through a polynomial-time exhaustive search among all candidate pairs $(\mathbf{b}, \mathbf{x})$.

C. Enumerating the locally optimal solutions of $\mathcal{P}_k$

To identify all intervals in $\left(-\frac{\pi}{2}, \frac{\pi}{2}\right]$ that retain their sign and amplitude vectors, it suffices to examine when *(i)* one of the curves that correspond to the elements of $\mathbf{u}(\phi)$ changes sign (i.e., when it becomes zero) or *(ii)* two of the curves that correspond to the elements of $|\mathbf{u}(\phi)|$ change their magnitude sorting (i.e., when two curves intersect). The second case is a necessary, but not sufficient, condition for a change in $\mathbf{b}_k(\phi) = \text{match}(k; \mathbf{u}(\phi))$, since the intersecting curves may correspond to elements of $|\mathbf{u}(\phi)|$ that are assigned to the same amplitude value a_m, $m = 1, 2, \ldots, \frac{M}{2}$. In the latter case, although the magnitude sorting of the curves changes, the amplitude vector $\mathbf{b}_k(\phi) = \text{match}(k; \mathbf{u}(\phi))$ does not.

When a curve, say $u_n(\phi)$, becomes zero, then

$$u_n(\phi) = 0 \Leftrightarrow V_{n,1} \sin\phi + V_{n,2} \cos\phi = 0 \Leftrightarrow \phi = \tan^{-1}\left(-\frac{V_{n,2}}{V_{n,1}}\right). \quad (34)$$

The solution in (34) determines a point (exactly where $u_n(\phi)$ changes sign) which partitions $\left(-\frac{\pi}{2}, \frac{\pi}{2}\right]$ into two intervals; in one of these intervals $u_n(\phi)$ is positive, while in the other interval it is negative. Since there are N curves $u_1(\phi)$, $u_2(\phi)$, $\ldots$, $u_N(\phi)$, we obtain N corresponding sign-change points through (34).

At the intersection of two curves, say $|u_n(\phi)|$ and $|u_l(\phi)|$, we have

$$|u_n(\phi)| = |u_l(\phi)| \Leftrightarrow V_{n,1}\sin(\phi) + V_{n,2}\cos(\phi) = \pm\left(V_{l,1}\sin(\phi) + V_{l,2}\cos(\phi)\right) \Leftrightarrow \phi = \tan^{-1}\left(\frac{\pm V_{l,2} - V_{n,2}}{V_{n,1} \mp V_{l,1}}\right). \quad (35)$$

The two solutions for ϕ in (35) determine two points that partition $\left(-\frac{\pi}{2}, \frac{\pi}{2}\right]$ into three intervals; in successive intervals, the inequality $|u_n(\phi)| > |u_l(\phi)|$ becomes $|u_n(\phi)| < |u_l(\phi)|$, or vice versa. These two points originate from a pair of elements of $|\mathbf{u}(\phi)|$. Since the N curves $|u_1(\phi)|, |u_2(\phi)|, \ldots, |u_N(\phi)|$ can be combined into $\binom{N}{2} = \frac{N^2 - N}{2}$ pairs and each pair yields two points, the number of points that correspond to intersections of curves in $\left(-\frac{\pi}{2}, \frac{\pi}{2}\right]$ equals $2\binom{N}{2} = N^2 - N$.

The aggregate number of sign- or sorting-change points in $\left(-\frac{\pi}{2}, \frac{\pi}{2}\right]$ is N^2. This means that $\left(-\frac{\pi}{2}, \frac{\pi}{2}\right]$ is partitioned into N^2 disjoint intervals and each such interval corresponds to a single amplitude-sign vector pair that remains unaltered within that interval.[4] Hence, the number of distinct locally optimal solutions of $\max_{\mathbf{b} \in \mathcal{B}_k} \max_{\mathbf{x} \in \{\pm 1\}^N} \left\{\mathbf{x}^T (\mathbf{b} \odot \mathbf{u}(\phi))\right\}$ generated for all values of $\phi \in \left(-\frac{\pi}{2}, \frac{\pi}{2}\right]$ is at most N^2. In the following subsection, we efficiently identify the candidate pairs $(\mathbf{b}, \mathbf{x})$.

D. Building the K candidate sets

In Fig. 3, we present the pseudo-code of our proposed detection algorithm that finds all candidate vectors for all $\mathcal{P}_k$, $k = 1, 2, \ldots, K$; for each step, we list the worst-case complexity.

All N^2 points in $\left(-\frac{\pi}{2}, \frac{\pi}{2}\right]$ where curves change signs or intersect are calculated at lines 2–8 and sorted at line 9. At line 10, we consider $\phi = -\frac{\pi}{2}$ and compute $\mathbf{x} = \text{sgn}\left(\mathbf{u}\left(-\frac{\pi}{2}\right)\right) = -\text{sgn}\left(\mathbf{V}_{:,1}\right)$. Then, at lines 11–20, we consider each value of $k = 1, 2, \ldots, K$ separately and make the following computations. At line 12, for $\phi = -\frac{\pi}{2}$ we find the locally optimal amplitude vector $\mathbf{b}_k = \text{match}\left(k; \mathbf{u}\left(-\frac{\pi}{2}\right)\right) = \text{match}\left(k; \mathbf{V}_{:,1}\right)$. The pair $(\mathbf{b}_k, \mathbf{x})$ (i.e., the signal vector $\mathbf{s}^{(k,1)} = \mathbf{b}_k \odot \mathbf{x}$ at line 13) is locally optimal for the interval that starts at $-\frac{\pi}{2}$ and ends at the first sign-change or intersection point from the sorted list. We continue by considering the first point from the sorted list, i.e., $i = 1$, and set $\mathbf{s}^{(k,2)}$ equal to $\mathbf{s}^{(k,1)}$ at line 15. If the

[4]The actual number of disjoint intervals is $N^2 + 1$. However, the first interval (that starts at $-\frac{\pi}{2}$) and the final interval (that ends at $\frac{\pi}{2}$) correspond to equal amplitude vectors $\mathbf{b}_k\left(-\frac{\pi}{2}\right) = \mathbf{b}_k\left(\frac{\pi}{2}\right)$ and opposite sign vectors $\mathbf{x}\left(-\frac{\pi}{2}\right) = -\mathbf{x}\left(\frac{\pi}{2}\right)$, resulting in equal metric value in $\mathcal{P}_k$ in (21). Hence, the final interval can be ignored.

ln.	Pseudocode	Complexity
1	$\mathbf{V} \leftarrow [\Re\{\mathbf{y}\} \ \Im\{\mathbf{y}\}]$	$\mathcal{O}(N)$
2	`for` $n = 1 : N$	
3	$\phi_n \leftarrow \tan^{-1}\left(-\frac{V_{n,2}}{V_{n,1}}\right)$	$\mathcal{O}(1)$
4	$i \leftarrow N$	$\mathcal{O}(1)$
5	`for` $n, l \in \{1, 2, \ldots, N\}$ `with` $n \neq l$	
6	$i \leftarrow i + 1$	$\mathcal{O}(1)$
7	$\phi_i \leftarrow \tan^{-1}\left(\frac{V_{l,2}-V_{n,2}}{V_{n,1}-V_{l,1}}\right)$	$\mathcal{O}(1)$
8	$\phi_{i+(N^2-N)/2} \leftarrow \tan^{-1}\left(\frac{-V_{l,2}-V_{n,2}}{V_{n,1}+V_{l,1}}\right)$	$\mathcal{O}(1)$
9	$[\phi_1, \phi_2, \ldots, \phi_{N^2}] \leftarrow$ `sort` $([\phi_1, \phi_2, \ldots, \phi_{N^2}])$	$\mathcal{O}(N \log N)$
10	$\mathbf{x} \leftarrow -\text{sgn}(\mathbf{V}_{:,1})$	$\mathcal{O}(N)$
11	`for` $k = 1 : K$	
12	$\mathbf{b}_k \leftarrow$ `match` $(k; \mathbf{V}_{:,1})$	$\mathcal{O}(N \log N)$
13	$\mathbf{s}^{(k,1)} \leftarrow \mathbf{b}_k \odot \mathbf{x}$	$\mathcal{O}(N)$
14	`for` $i = 1 : N^2 - 1$	
15	$\mathbf{s}^{(k,i+1)} \leftarrow \mathbf{s}^{(k,i)}$	$\mathcal{O}(N)$
16	`if` ϕ_i `is a` $u_n(\phi_i) = 0$ `root`	
17	$s_n^{(k,i+1)} \leftarrow -s_n^{(k,i)}$	$\mathcal{O}(1)$
18	`if` ϕ_i `is a` $\lvert u_n(\phi_i)\rvert = \lvert u_l(\phi_i)\rvert$ `root`	
19	$s_n^{(k,i+1)} \leftarrow \text{sgn}\left(s_n^{(k,i)}\right)\left\lvert s_l^{(k,i)}\right\rvert$	$\mathcal{O}(1)$
20	$s_l^{(k,i+1)} \leftarrow \text{sgn}\left(s_l^{(k,i)}\right)\left\lvert s_n^{(k,i)}\right\rvert$	$\mathcal{O}(1)$

Fig. 3. The algorithm that builds the candidate vector set.

point ϕ_1 that we consider corresponds to a sign change, then, at line 17, we update $\mathbf{s}^{(k,2)}$ by switching the sign of its element that corresponds to the curve that changes sign. Otherwise, ϕ_1 is an intersection point, hence we consider the indices n, l of the two curves that intersect and, at lines 19 and 20, switch the amplitudes of elements n and l in $\mathbf{s}^{(k,2)}$. Next, we move to the next point from the sorted list (i.e., $i = 2$), set $\mathbf{s}^{(k,3)}$ equal to $\mathbf{s}^{(k,2)}$, and repeat the above procedure, i.e., update a sign or two amplitudes of $\mathbf{s}^{(k,3)}$ if the point ϕ_2 that we consider corresponds to a sign change or an intersection, respectively. We continue similarly until we visit all N^2 points except from the last one. In the end, for each $k = 1, 2, \ldots, K$, we have collected a set of at most N^2 distinct candidate vectors $\mathbf{s}^{(k,i)}$ with $i = 1, \ldots, N^2$.

For brevity and presentation clarity, in the algorithm of Fig. 3 we have omitted the calculation of the metric

$$g(\|\mathbf{s}\|)\left\|\mathbf{V}^T\mathbf{s}\right\|^2 + h(\|\mathbf{s}\|) \tag{36}$$

in $\mathcal{P}$ (cf. (11)). However, for each $k = 1, 2, \ldots, K$, we can calculate the first vector $\mathbf{s}^{(k,1)}$ with complexity $\mathcal{O}(N) + \mathcal{O}(N \log N)$ and its corresponding metric with complexity $\mathcal{O}(N)$ since $\mathbf{V}$ is an $N \times 2$ matrix. Then, to update the metric for $\mathbf{s}^{(k,2)}$, we only need to recalculate the matrix product for the coefficients that have changed, which costs $\mathcal{O}(1)$. If the metric for this vector is strictly higher than that of $\mathbf{s}^{(k,1)}$, then we keep it as a candidate. We continue similarly for all $\mathbf{s}^{(k,2)}$, $\mathbf{s}^{(k,3)}$, $\ldots$, $\mathbf{s}^{(k,N^2)}$. That is, for any $k = 1, 2, \ldots, K$, the worst-case complexity for the generation of the solution of $\mathcal{P}_k$ is $\mathcal{O}(N^2)$. Hence, we have the following lemma.

Lemma 2: The optimal solution of $\mathcal{P}_k$ can be calculated in time $\mathcal{O}(N^2)$. □

In the end, we keep K candidate vectors which are the solution vectors of $\mathcal{P}_1, \mathcal{P}_2, \ldots, \mathcal{P}_K$. We compare their metric evaluations (which cost $\mathcal{O}(N)$ each) and keep the one with the largest one; that is exactly the optimal solution vector of $\mathcal{P}$. Hence, the optimization metric for $\mathcal{P}$ in (11) can be calculated in time $\mathcal{O}(NK)$ for the candidate vectors generated by the algorithm of Fig. 3. The overall complexity of the proposed solution is dominated by the computational cost needed to generate the candidate vectors $\mathbf{s}^{(k,i)}$ with $k = 1, 2, \ldots, K$ and $i = 1, \ldots, N^2$. Hence, from Lemmas 1 and 2, we conclude that the worst-case overall complexity of the proposed solution of $\mathcal{P}$ is $\mathcal{O}\left(N^{\frac{M}{2}+1}\right)$, which proves Proposition 1.

IV. Extension to QAM

For simplicity of the presentation, we concentrated our analysis and developments to PAM transmissions, as described in (1) and (2). In the case of QAM, with a slight modification that is presented below, our proposed algorithm still solves, with polynomial complexity, the optimization problem $\mathcal{P}$ in (11), hence the ML and GLRT noncoherent sequence detection problems.

We recall that, for M-PAM, the ML and GLRT sequence detection problems are special case of (11). The two important quantities in the proof of (11) are $\mathbf{y}^H\mathbf{s}$ and $\|\mathbf{s}\|$. In the case of M-QAM, the transmitted signal vector takes the form

$$\mathbf{s} = \mathbf{s}_\Re + j\mathbf{s}_\Im = [\mathbf{I} \ \ j\mathbf{I}]\begin{bmatrix}\mathbf{s}_\Re \\ \mathbf{s}_\Im\end{bmatrix} \tag{37}$$

where the $\sqrt{M}$-PAM vectors $\mathbf{s}_\Re \in \mathcal{A}_{\sqrt{M}}$ and $\mathbf{s}_\Im \in \mathcal{A}_{\sqrt{M}}$ are the real and imaginary, respectively, parts of the M-QAM vector $\mathbf{s}$. We define the $\sqrt{M}$-PAM vector $\tilde{\mathbf{s}} \stackrel{\triangle}{=} \left[\mathbf{s}_\Re^T \ \ \mathbf{s}_\Im^T\right]^T$ of length $2N$. Then, (37) becomes

$$\mathbf{s} = [\mathbf{I} \ \ j\mathbf{I}]\,\tilde{\mathbf{s}} \tag{38}$$

and the two quantities that affect the proof of (11) become

$$\|\mathbf{s}\| = \|\tilde{\mathbf{s}}\| \tag{39}$$

and

$$\mathbf{y}^H\mathbf{s} = \mathbf{y}^H[\mathbf{I} \ \ j\mathbf{I}]\,\tilde{\mathbf{s}} = \left[\mathbf{y}^H \ \ j\mathbf{y}^H\right]\tilde{\mathbf{s}} = \tilde{\mathbf{y}}^H\tilde{\mathbf{s}} \tag{40}$$

where $\tilde{\mathbf{y}} \stackrel{\triangle}{=} \left[\mathbf{y}^T \ \ -j\mathbf{y}^T\right]^T \in \mathbb{C}^{2N}$. From (39) and (40), it turns out that the ML (or GLRT) noncoherent detection of an M-QAM sequence of length N simplifies to the ML (or GLRT) noncoherent detection of an equivalent $\sqrt{M}$-PAM sequence of length $2N$. Hence, the optimal M-QAM sequence of length N is obtained by the proposed algorithm with worst-case complexity $\mathcal{O}\left(N^{\frac{\sqrt{M}}{2}+1}\right)$.

V. Simulation Results

As an illustration, we consider PAM transmissions in an unknown Rayleigh fading channel environment and present the symbol error rate (SER) of the GLRT and ML sequence detectors as a function of the transmitted signal-to-noise ratio (SNR). The presented results are averaged over 250 channel realizations.

In Fig. 4, we present results for 4-PAM and sequence length $N = 6$, 10, and 18. We note that GLRT detection

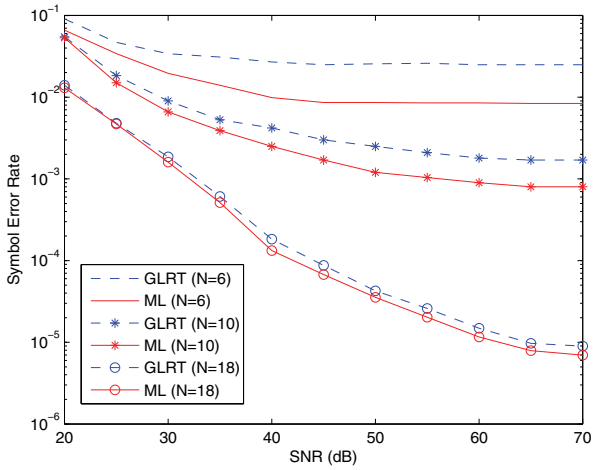

Fig. 4. 4-PAM symbol error rate versus SNR for GLRT and ML noncoherent receivers with sequence length $N = 6$, 10, and 18.

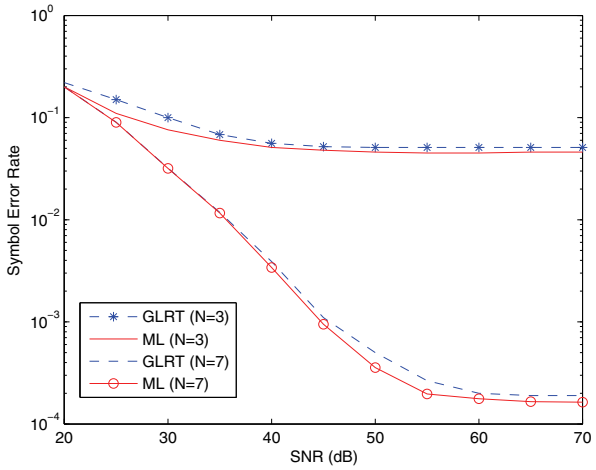

Fig. 6. 16-QAM symbol error rate versus SNR for GLRT and ML noncoherent receivers with sequence length $N = 3$ and 7.

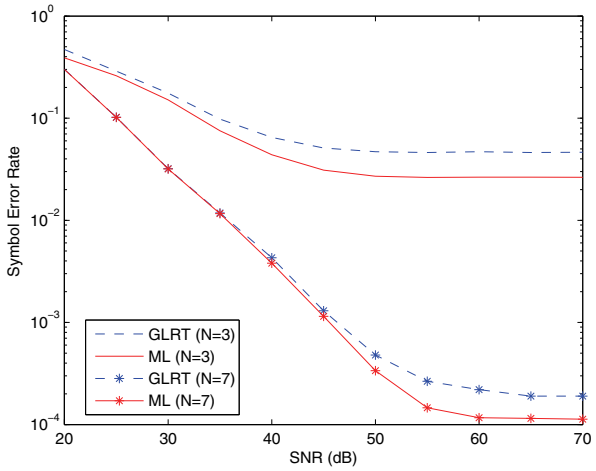

Fig. 5. 8-PAM symbol error rate versus SNR for GLRT and ML noncoherent receivers with sequence length $N = 3$ and 7.

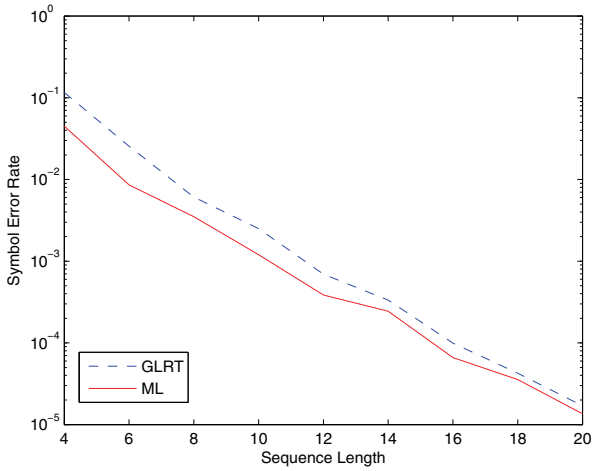

Fig. 7. 4-PAM symbol error rate versus sequence length N for GLRT and ML noncoherent receivers and SNR = 50dB.

is implemented by the algorithm developed in [12], [13] with complexity $\mathcal{O}\left(N^2 \log N\right)$ while ML detection is implemented by the proposed algorithm with complexity $\mathcal{O}\left(N^3\right)$. We observe performance gains of ML detection over GLRT detection, for all three values of the sequence length. These gains result solely from the fact that the ML detector is tailored to the Rayleigh fading environment.

In Fig. 5, we present results for 8-PAM and sequence length $N = 3$ and 7. Here, GLRT detection has the same complexity as in 4-PAM while ML detection requires $\mathcal{O}\left(N^5\right)$ computational cost. The performance gains of ML detection over GLRT detection are maintained. In Fig. 6, we present a similar study for 16-QAM and sequence length $N = 3$ and 7. In this case, the complexity is the same as in 4-PAM, i.e., $\mathcal{O}\left(N^2 \log N\right)$ for the GLRT receiver and $\mathcal{O}\left(N^3\right)$ for the ML receiver.

Finally, in Fig. 7, we consider 4-PAM transmissions, set the SNR to 50dB, and plot the SER of GLRT and ML detectors as a function of the sequence length N. We note that the performance of both detectors improves as the sequence length increases and, interestingly, GLRT detection attains near-ML performance for very large values of N.

VI. Conclusions

In this work, we developed a method for ML noncoherent detection of M-PAM/QAM symbol sequences under Rayleigh fading whose complexity is polynomial in the sequence length when M is constant. Our approach decomposes the detection problem into a polynomial-size set of simple problems. This is possible through an auxiliary-angle approach which, in principle, rephrases a computationally hard exhaustive-search problem into one that has to run on a polynomial-size search set, by unlocking a low-rank property of the ML detection problem. We showed that this new set is built with polynomial complexity in the sequence length and always contains the ML PAM/QAM sequence.

To keep the presentation simple, we focused on PAM transmissions and presented the properties of our algorithm accompanied by a detailed worst-case complexity analysis. It is straightforward to extend the presented algorithm to ML

noncoherent detection of QAM sequences without increasing its worst-case complexity order.

Interestingly, the ML and GLRT noncoherent PAM/QAM detection problems are special cases of a more general optimization problem defined over any finite alphabet (that does not necessarily consist of pair-wise opposite elements, as considered in this work). This more general optimization problem can be always solved in polynomial time by the presented approach.

REFERENCES

[1] T. L. Marzetta and B. M. Hochwald, "Capacity of a mobile multiple-antenna communication link in Rayleigh flat fading," *IEEE Trans. Inf. Theory*, vol. 45, pp. 139–157, Jan. 1999.

[2] L. Zheng and D. N. C. Tse, "Communication on the Grassmann manifold: a geometric approach to the noncoherent multiple-antenna channel," *IEEE Trans. Inf. Theory*, vol. 48, pp. 359–383, Feb. 2002.

[3] R.-R. Chen, R. Koetter, U. Madhow, and D. Agrawal, "Joint noncoherent demodulation and decoding for the block fading channel: a practical framework for approaching Shannon capacity," *IEEE Trans. Commun.*, vol. 51, pp. 1676–1689, Oct. 2003.

[4] D. Makrakis and P. T. Mathiopoulos, "Optimal decoding in fading channels: a combined envelope, multiple differential and coherent detection approach," in *Proc. 1989 IEEE GLOBECOM*, vol. 3, pp. 1551–1557.

[5] S. G. Wilson, J. Freebersyser, and C. Marshall, "Multi-symbol detection of M-DPSK," in *Proc. 1989 IEEE GLOBECOM*, vol. 3, pp. 1692–1697.

[6] D. Divsalar and M. K. Simon, "Multiple-symbol differential detection of MPSK," *IEEE Trans. Commun.*, vol. 38, pp. 300–308, Mar. 1990.

[7] K. M. Mackenthun, Jr., "A fast algorithm for multiple-symbol differential detection of MPSK," *IEEE Trans. Commun.*, vol. 42, pp. 1471–1474, Feb./Mar./Apr. 1994.

[8] W. Sweldens, "Fast block noncoherent decoding," *IEEE Commun. Lett.*, vol. 5, pp. 132–134, Apr. 2001.

[9] I. Motedayen-Aval, A. Krishnamoorthy, and A. Anastasopoulos, "Optimal joint detection/estimation in fading channels with polynomial complexity," *IEEE Trans. Inf. Theory*, vol. 53, pp. 209–223, Jan. 2007.

[10] G. N. Karystinos and D. A. Pados, "Rank-2-optimal adaptive design of binary spreading codes," *IEEE Trans. Inf. Theory*, vol. 53, pp. 3075–3080, Sept. 2007.

[11] I. Motedayen-Aval and A. Anastasopoulos, "Polynomial-complexity noncoherent symbol-by-symbol detection with application to adaptive iterative decoding of turbo-like codes," *IEEE Trans. Commun.*, vol. 51, pp. 197–207, Feb. 2003.

[12] D. J. Ryan, I. B. Collings, and I. V. L. Clarkson, "GLRT-optimal noncoherent lattice decoding," *IEEE Trans. Signal Process.*, vol. 55, pp. 3773–3786, July 2007.

[13] R. G. McKilliam, D. J. Ryan, I. V. L. Clarkson, and I. B. Collings, "An improved algorithm for optimal noncoherent QAM detection," in *Proc. 2008 Australian Commun. Theory Workshop*, pp. 64-68.

[14] C. D. Meyer, *Matrix Analysis and Applied Linear Algebra*. SIAM, 2000.

[15] T. M. Cover and J. A. Thomas, *Elements of Information Theory*, 2nd edition. Wiley, 2006.

[16] R. P. Stanley, *Enumerative Combinatorics, Volume 1*, 2nd edition. Cambridge University Press, 2012.

Dimitris S. Papailiopoulos (S'10) received the Diploma (five-year program) and M.Sc. degrees in electronic and computer engineering from the Technical University of Crete, Chania, Greece, in 2007 and 2009, respectively. He is currently working toward the Ph.D. degree at the Department of Electrical Engineering, University of Southern California, Los Angeles. His research interests are in the areas of coding theory, signal processing, and optimization theory, with an emphasis on codes for distributed storage, interference alignment, and combinatorial optimization. Mr. Papailiopoulos is the recipient of the Annenberg Fellowship in 2009 and the Myronis Fellowship in 2011, both from the Graduate School of the University of Southern California.

Georgina Abou Elkheir received the Diploma (five-year program) and M.Sc. degrees in electronic and computer engineering from the Technical University of Crete, Chania, Greece, in 2007 and 2011, respectively. She is currently working toward the Ph.D. degree at the Department of Digital Systems, University of Piraeus, Greece supported in part by the European Union's Seventh Framework Programme Integrating Project EXALTED - Expanding LTE for devices. Her current research interests are in the general areas of communication theory with emphasis on wireless and cooperative communications, resource allocation, and cross-layer design.

George N. Karystinos (S'98-M'03) was born in Athens, Greece, on April 12, 1974. He received the Diploma degree in computer science and engineering (five-year program) from the University of Patras, Patras, Greece, in 1997 and the Ph.D. degree in electrical engineering from the State University of New York at Buffalo, Amherst, NY, in 2003. In August 2003, he joined the Department of Electrical Engineering, Wright State University, Dayton, OH as an Assistant Professor. Since September 2005, he has been an Assistant Professor with the Department of Electronic and Computer Engineering, Technical University of Crete, Chania, Greece. His current research interests are in the general areas of communication theory and adaptive signal processing with an emphasis on wireless and cooperative communications systems, low-complexity sequence detection, optimization with low complexity and limited data, spreading code and signal waveform design, and sparse principal component analysis.

Dr. Karystinos received a 2001 IEEE International Conference on Telecommunications best paper award, the 2003 IEEE Transactions on Neural Networks Outstanding Paper Award, and the 2011 IEEE International Conference on RFID-Technologies and Applications Second Best Student Paper Award. He is a member of the IEEE Communications, Signal Processing, Information Theory, and Computational Intelligence Societies and a member of Eta Kappa Nu.